Effect of Co addition for carburizing process of Ti-oxide/SiO2 into TiC/SiO2

Yasuhiro Iwama [a], Nobuyuki Ichikuni [a,*], Kyoko K. Bando [b], Shogo Shimazu [a]

[a] Department of Applied Chemistry and Biotechnology, Faculty of Engineering, Chiba University, Inage-ku, Chiba 263-8522, Japan
[b] National Institute of Advanced Industrial Science and Technology, Tsukuba, Ibaraki 305-8569, Japan

Abstract

Lowering the carburization temperature of Ti-oxide into TiC down to 1173 K could be achieved by the addition of Co. Co-promoted TiC/SiO2 catalysts were prepared by the temperature programmed reaction (TPR) method. Co–Ti/SiO2 precursors were prepared by use of the successive impregnation method (sc) and the co-impregnation method (co). Samples were characterized by X-ray absorption fine structure (XAFS) measurements and X-ray diffraction (XRD) results. The carburization degree of TiC was affected by the method of Co addition. The carburization degree of sc Co–TiC/SiO2 was better than that of co Co–TiC/SiO2. The activity of thiophene hydrodesulfurization reaction at 693 K on sc Co–TiC/SiO2 was higher than that on co Co–TiC/SiO2. The HDS activity was related to the carburization degree of TiC.
© 2007 Elsevier B.V. All rights reserved.

Keywords: TiC catalyst; XAFS; Co additive; Carburization

1. Introduction

Small atoms, such as carbon or nitrogen, dissolved interstitially in the lattices of early transition metals produce a class of compounds with unique physical and chemical properties [1,2]. These interstitial compounds are referred to as early transition metal carbides (ETMC) and nitrides (ETMN). ETMC and ETMN were found to have similar activities to those of the group 8–10 metals (Pt, Pd, Rh, etc.) [3–6].

Most of works on the catalytic applications of ETMC have been focused on Mo2C and WC [7–10]. In contrast, very few works have been reported on the groups 4 and 5 metal carbides such as TiC and NbC [11–14]. The focus on Mo2C and WC has occurred in part because they could be prepared with high surface areas at moderate synthesis temperatures in the range between 900 K and 1100 K [7–10]. On the other hand, it has been reported that the carburization of bulk TiO2 into TiC requires a high temperature; 1410 K [5]. Using high temperature caused a sintering of TiC, and decreased the surface area of TiC. The lowering of carburizing temperature is required for the catalytic application of TiC. We have demonstrated that the carburizing temperature could be lowered by supporting the metal species on amorphous silica [15,16].

Co addition could be expected to promote the carburization with activating methane by dehydrogenation because it has been used for Fischer–Tropsch catalysts [17]. In this work, in order to lower carburization temperature, we added Co to TiO2, and then demonstrated carburization. In addition, Co–TiC/SiO2 was prepared. For the preparation of Co–Ti/SiO2, two different methods were applied. One is successive impregnation method (sc), and the other is co-impregnation method (co). Co–Ti/SiO2 precursors were carburized by using temperature programmed reaction (TPR) method. Carburization degree of Ti was characterized by using Ti K-edge XAFS (X-ray absorption fine structure) measurements. In order to investigate the effect of Co addition, Co K-edge XAFS was also measured. Thiophene HDS (hydrodesulfurization) reactions were demonstrated to investigate the relationship between the carburization degree of TiC activity and the HDS.

2. Experimental

Co–Ti/SiO2 precursors were prepared by sc method (sc Co–Ti/SiO2) and co method (co Co–Ti/SiO2). The preparation

* Corresponding author. Tel.: +81 43 290 3380; fax: +81 43 290 3401.
E-mail address: ichikuni@faculty.chiba-u.jp (N. Ichikuni).

process of sc Co–Ti/SiO$_2$ consisted of two stages. First, intermediate precursors of Ti/SiO$_2$ were obtained by impregnating SiO$_2$ (Aerosil, #200) with TiCl$_4$/HCl solutions at RT for 24 h. To decompose the titanium chloride, we calcined the intermediate precursor at 623 K in air for 2 h. Second, Co–Ti/SiO$_2$ was obtained by impregnating Ti/SiO$_2$ with aqueous cobalt chloride solution at RT for 24 h. To decompose the cobalt chloride, we calcined the precursor at 623 K in air for 2 h. Ti loading was regulated to 5 wt% with a Co/Ti molar ratio of 0.25. The co-impregnation catalyst was prepared as follows: an HCl aqueous solution of TiCl$_4$ and CoCl$_2$ was impregnated with SiO$_2$ at RT for 24 h. To decompose the titanium chloride and the cobalt chloride, we calcined the precursor at 623 K in air for 2 h (co Co–Ti/SiO$_2$).

The Co–Ti/SiO$_2$ precursor was carburized in a 20% CH$_4$/H$_2$ mixed gas stream to produce Co–TiC/SiO$_2$ in the TPR process. This process involves two steps: (1) raising the temperature at a linear rate of 10 K min^{-1} to 1273 K and (2) maintaining the sample at the final temperature for a certain period.

XAFS spectra at Ti K-edge and Co K-edge were measured at RT in transmission mode at BL-10B (Co K-edges), BL-7C, 9C and 12C (Ti K-edges) using the Photon Factory in the Institute of Material Structure Science, High Energy Accelerator Research Organization (PF, IMSS-KEK) (Proposals nos. 2002G116, 2005G214). Synchrotron radiation emitted from a 2.5 GeV storage ring was monochromatized by a Si(3 1 1) channel cut monochromator or a Si(1 1 1) double crystal monochromator at BL-10B or BL-7C, 9C, 12C, respectively. Each sample was pressed into a pellet, which was 10 mm in diameter. Curve-fitting analysis of EXAFS oscillations was conducted by the EXAFS analysis program REX2000 (Rigaku Co.). Model parameters for curve-fitting analysis (back scattering amplitude and phase shift functions) were extracted from EXAFS oscillations observed for standard materials (TiO$_2$, TiC, CoTiO$_3$, Co foil, Co$_3$O$_4$ and CoS), or they were created by FEFF.

The XRD (X-ray diffraction) analysis (Bruker axs, MXP3) was also carried out. HDS of thiophene was performed in continuous flow system interfaced to a gas chromatograph (SHIMADZU, GC-8A) with a TCD detector. The main products were 1-butene and 2-butene. The catalyst (0.4 g) was pretreated under H$_2$ flow (10 ml min^{-1}) for 0.5 h at 1073 K or 773 K, prior to use. HDS reaction was monitored under 2.8% thiophene/H$_2$ (5 ml min^{-1}) at 693 K.

3. Results and discussion

3.1. Carburization of bulk TiO$_2$

XRD patterns of TiO$_2$, TiC, carburized TiO$_2$ and carburized Co–TiO$_2$ are shown in Fig. 1. In the case of carburized TiO$_2$, the Ti$_3$O$_5$ phase was observed and no peak attributed to TiC was appeared. On the other hand, the patterns for carburized Co–TiO$_2$ showed TiC phase clearly. Such results mean that TiO$_2$ was not carburized at 1273 K without Co additive, but was carburized to produce TiC with Co additive. In the case of carburized Co–TiO$_2$, Co metal phase was observed as well as
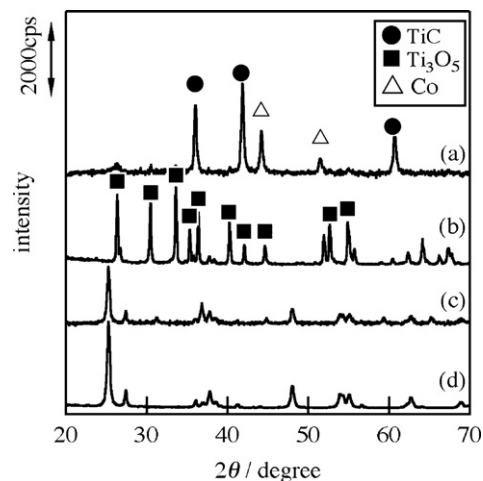

Fig. 1. XRD patterns of (a) carburized Co–TiO$_2$, (b) carburized TiO$_2$, (c) Co–TiO$_2$ and (d) bulk TiO$_2$.

TiC phase. It was found that Co oxide was reduced to Co metal during the carburization. We supposed that the carburization of TiO$_2$ proceeded focusing around reduced Co.

In order to optimize the carburization condition, we prepared carburized Co–TiO$_2$ by controlling the carburization temperature and the retention time. Fig. 2 shows XRD patterns of carburized Co–TiO$_2$ as a function of carburization temperature (1273 K, 1223 K, 1173 K and 1073 K). The XRD pattern of Co–TiO$_2$ carburized at 1073 K shows only Ti$_3$O$_5$ phase. It can be said that TiC was not formed by a carburization temperature as low as 1073 K. In the case of Co–TiO$_2$ carburized at 1173 K, however, TiC phase was observed slightly besides the main Ti$_3$O$_5$ phase. It was found that TiC was formed by the carburization above 1173 K. In other words, the carburization temperature of Ti-oxide into TiC could be lowered down to 1173 K by addition of Co. In the case of Co–TiO$_2$ carburized at 1223 K, the TiC phase was larger compared to the case of Co–TiO$_2$ carburized at 1173 K. Raising the carburization temperature up to 1273 K, we could distinctly observe the TiC phase
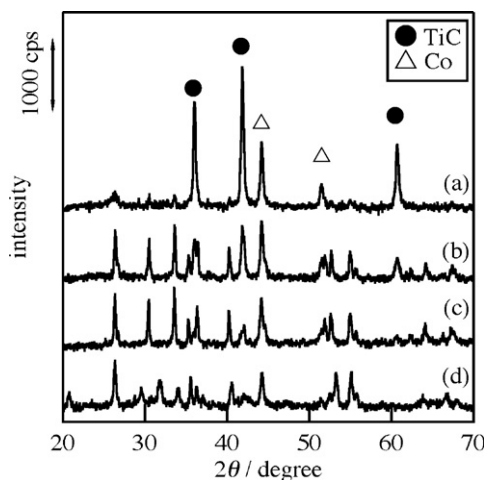

Fig. 2. XRD patterns of carburized Co–TiO$_2$ varied with the carburization temperature: (a) 1273 K, (b) 1223 K, (c) 1173 K and (d) 1073 K.
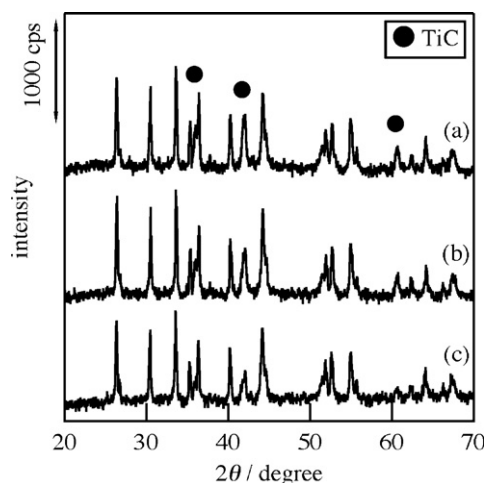
Fig. 3. XRD patterns of carburized Co–TiO₂ (carburization temperature = 1173 K) maintained for (a) 120 min, (b) 80 min and (c) 40 min.

and the Ti₃O₅ phase disappeared. The carburization degree from Ti-oxide to TiC became higher as the carburization temperature increased. Fig. 3 shows that XRD patterns of carburized Co–TiO₂ (carburization temperature = 1173 K) varied with the retention time (40 min, 80 min and 120 min). They included Ti₃O₅ phase and very weak TiC phase. Almost no differences are found among the three samples. It was supposed that the retention time has less dependence on the carburization degree compared to the carburization temperature.

3.2. Carburization of TiO₂/SiO₂

In the supported system, the carburization condition was regulated as follows: the carburization temperature is 1273 K and the retention time is 30 min. Co-promoted TiC/SiO₂ catalysts were prepared by the carburization of Co–Ti/SiO₂ precursors.

Ti K-edge XAFS measurements were carried out to determine the electronic state and the local structure of the
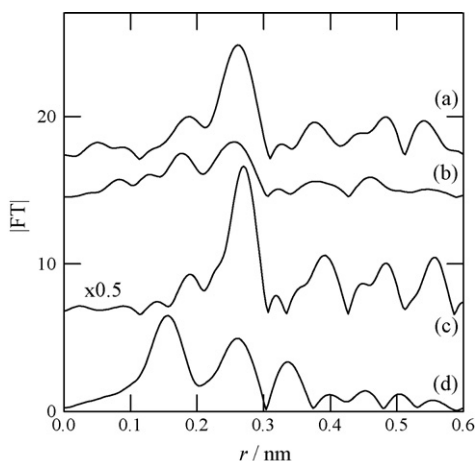
Table 1
Curve-fitting results for Ti–C and Ti–(C)–Ti coordination on Co–TiC/SiO₂ catalysts

Sample	Coordination	CN	r (nm)	dE_0 (eV)	DW (nm)
sc Co–TiC/SiO₂	Ti–C	3.6	0.212	−4.07	0.0067
	Ti–(C)–Ti	6.1	0.303	−4.96	0.0070
co Co–TiC/SiO₂	Ti–C	2.0	0.205	12.60	0.0054
	Ti–O	1.2	0.212	−16.21	0.0073
	Ti–(C)–Ti	3.2	0.301	−8.95	0.0072
Bulk TiC (model)	Ti–C	6	0.217	0	0.0060
	Ti–(C)–Ti	12	0.306	0	0.0060

catalysts. Fig. 4 shows the FT (Fourier transform) of k^3-weighted EXAFS oscillations for Co–TiC/SiO₂ catalysts. CF (curve-fitting) analysis was carried out by using the bulk TiC as the reference compound to determine CN (coordination number) and the coordination distance. FT profiles of both sc Co–TiC/SiO₂ and co Co–TiC/SiO₂ are similar to that of bulk TiC. The CF results are listed in Table 1. CN values of Ti–C and Ti–O were different for sc Co–TiC/SiO₂ and for co Co–TiC/SiO₂. In the case of sc Co–TiC/SiO₂, CN values of Ti–C and Ti–O were 3.6 and 0.0, respectively. In the case of co Co–TiC/SiO₂, however, CN values of Ti–C and Ti–O were 2.0 and 1.2, respectively. It was found that Ti-oxide was still remained on co Co–TiC/SiO₂. It was supposed that the carburization degree of sc Co–TiC/SiO₂ was better than that of co Co–TiC/SiO₂. CN values of Ti–(C)–Ti for sc Co–TiC/SiO₂ and co Co–TiC/SiO₂ were 6.1 and 3.2, respectively. CN of Ti–(C)–Ti correlates with the TiC particle size. And hence, the particle size of sc Co–TiC/SiO₂ seems to be larger than that of co Co–TiC/SiO₂. CN values of Ti–(C)–Ti coordination for both Co–TiC/SiO₂ were less than that for bulk TiC (CN = 12). It was suggested that TiC on Co–TiC/SiO₂ were highly dispersed on the SiO₂ surface. To explain the difference of the carburization degree, we carried out Ti K-edge XAFS measurements for Co–Ti/SiO₂ precursor. Fig. 5 shows the FT of k^3-weighted EXAFS oscillations for Co–Ti/SiO₂ precursors. CF analysis was carried out by using the bulk

Fig. 4. Fourier transforms of k^3-weighted Ti K-edge EXAFS oscillations for (a) sc Co–TiC/SiO₂, (b) co Co–TiC/SiO₂, (c) TiC and (d) TiO₂.
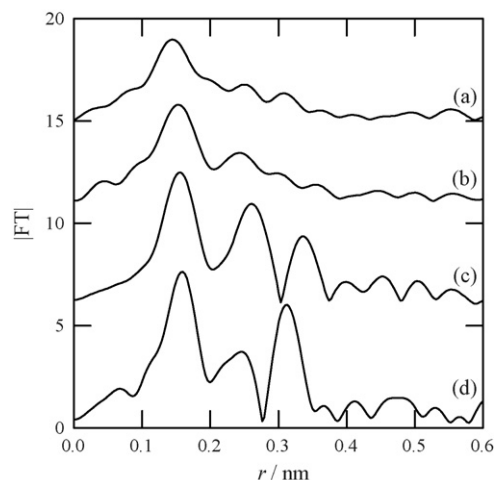

Fig. 5. Fourier transforms of k^3-weighted Ti K-edge EXAFS oscillations for (a) sc Co–Ti/SiO₂, (b) co Co–Ti/SiO₂, (c) TiO₂ (anatase) and (d) TiO₂ (rutile).

Table 2
Curve-fitting results for Ti–O and Ti–(O)–Ti coordination on Co–Ti/SiO$_2$ catalysts

Sample	Coordination	CN	r (nm)	dE_0 (eV)	DW (nm)
sc Co–Ti/SiO$_2$	Ti–O	3.7	0.190	−3.12	0.0072
	Ti–(O)–Ti	1.4	0.301	−12.42	0.0073
	Ti–(O)–Ti	1.4	0.345	6.24	0.0068
co Co–Ti/SiO$_2$	Ti–O	3.8	0.191	−6.02	0.0064
	Ti–(O)–Ti	2.3	0.296	−16.86	0.0081
	Ti–(C)–Ti	1.6	0.345	3.88	0.0067
Bulk TiO$_2$ (model, anatase)	Ti–O	6	0.196	0	0.0060
	Ti–(O)–Ti	4	0.304	0	0.0060
	Ti–(O)–Ti	4	0.379	0	0.0060

Table 3
Curve-fitting results for Co–O, Co–(O)–Co and Co–(O)–Ti coordination on Co–Ti/SiO$_2$ catalysts

Sample	Coordination	CN	r (nm)	dE_0 (eV)	DW (nm)
sc Co–Ti/SiO$_2$	Co–O	4.9	0.197	−2.75	0.0058
	Co–(O)–Co	3.1	0.286	5.76	0.0062
	Co–(O)–Co	2.9	0.336	5.47	0.0054
co Co–Ti/SiO$_2$	Co–O	5.1	0.197	−20.41	0.0098
	Co–(O)–Ti	0.86	0.350	−5.79	0.0056
	Co–(O)–Ti	0.97	0.405	−10.46	0.0051
Bulk Co$_3$O$_4$ (model)	Co–O	1.3	0.181	0	0.0060
	Co–O	4	0.199	0	0.0060
	Co–(O)–Co	4	0.287	0	0.0060
Bulk CoTiO$_3$ (model)	Co–O	6	0.214	0	0.0060
	Co–(O)–Ti	6	0.253	0	0.0060
	Co–(O)–Ti	6	0.273	0	0.0060

TiO$_2$ as the reference compound [18]. The results are listed in Table 2. Both Co–Ti/SiO$_2$ precursors showed structures similar to that of rutile TiO$_2$. It was found that Ti species in Co–Ti/SiO$_2$ precursor are in the rutile phase TiO$_2$, and no clear difference was observed between sc Co–Ti/SiO$_2$ and co Co–Ti/SiO$_2$ precursors. The carburization degree of TiO$_2$ was affected not by the phase of precursor TiO$_2$, but by the state of concomitant Co. Thus, Co K-edge XAFS measurements were carried out for Co–Ti/SiO$_2$ precursor (Table 3).

Fig. 6 shows Co K-edge XANES spectra of Co–Ti/SiO$_2$ precursors, Co$_3$O$_4$ and CoTiO$_3$. A strong absorption band around 7730 eV and 7725 eV was observed in XANES spectra for Co$_3$O$_4$ and CoTiO$_3$, respectively. From the XANES profile, the states of Co in sc Co–Ti/SiO$_2$ and co Co–Ti/SiO$_2$ were similar to those in Co$_3$O$_4$ and CoTiO$_3$, respectively.

Fig. 7 shows Co K-edge XANES spectra of Co–TiC/SiO$_2$ and Co foil. The XANES profiles of Co–TiC/SiO$_2$ catalysts were more similar to that of Co foil than to that of Co oxide. It was supposed that Co oxide was reduced to the metal for Co–TiC/SiO$_2$ during the carburization process. No difference was observed in XANES profiles between sc Co–TiC/SiO$_2$ and co Co–TiC/SiO$_2$. Since the XANES profile of Co–TiC/SiO$_2$ differed from that of Co foil at around 7745 eV, it was supposed that Co of Co–TiC/SiO$_2$ was in the Co–Ti alloy or CoC$_x$ species [19].

Fig. 8 shows the FT of k^3-weighted Co K-edge EXAFS oscillations for Co–Ti/SiO$_2$ precursor. The FT profile of sc Co–

Ti/SiO$_2$ resembled that of bulk Co$_3$O$_4$. On the other hand, the FT profile of co Co–Ti/SiO$_2$ was not similar to that of Co$_3$O$_4$ but was close to that of CoTiO$_3$. CF analysis was carried out by using bulk Co$_3$O$_4$ and CoTiO$_3$ as the reference compound [20]. The CN (Co–(O)–Co) of sc Co–Ti/SiO$_2$ (3.1) was less than that of Co$_3$O$_4$ (4.0). It was supposed that Co$_3$O$_4$ on sc Co–Ti/SiO$_2$ was dispersed, and that small Co$_3$O$_4$ clusters were formed at the TiO$_2$ surface. In the case of co Co–Ti/SiO$_2$, CN (Co–(O)–Ti)
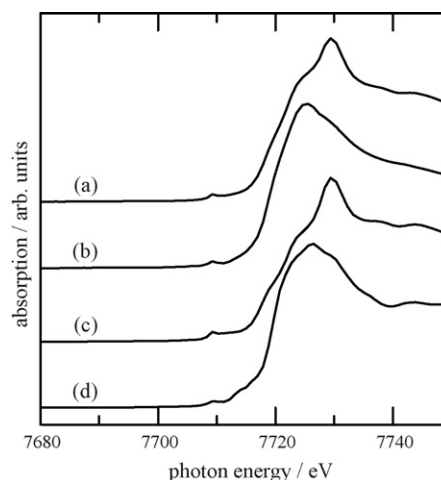

Fig. 6. Co K-edge XANES spectra of (a) sc Co–Ti/SiO$_2$, (b) co Co–Ti/SiO$_2$, (c) Co$_3$O$_4$ and (d) CoTiO$_3$.
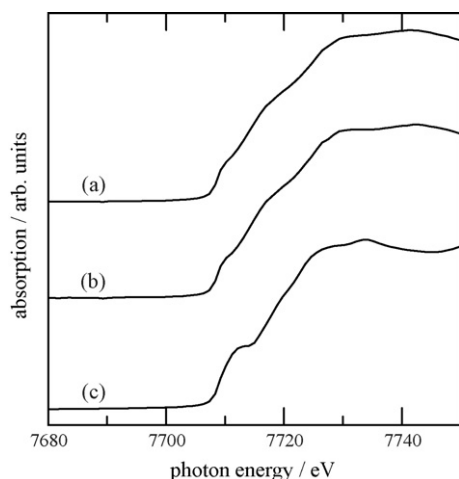
Fig. 7. Co K-edge XANES spectra of (a) sc Co–TiC/SiO$_2$, (b) co Co–TiC/SiO$_2$ and (c) Co foil.

Fig. 9. Fourier transforms of k^3-weighted Co K-edge EXAFS oscillations for (a) sc Co–TiC/SiO$_2$, (b) co Co–TiC/SiO$_2$ and (c) Co foil.
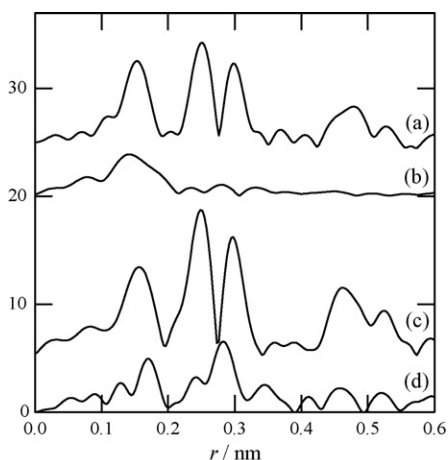

Fig. 8. Fourier transforms of k^3-weighted Co K-edge EXAFS oscillations for (a) sc Co–Ti/SiO$_2$, (b) co Co–Ti/SiO$_2$, (c) Co$_3$O$_4$ and (d) CoTiO$_3$.

Scheme 1. Plausible structure of carburization process from sc Co–Ti/SiO$_2$ into sc Co–TiC/SiO$_2$.

was much less than that of CoTiO$_3$. It was supposed that CoTiO$_3$ on co Co–Ti/SiO$_2$ was highly dispersed, formed at the surface and the inside of TiO$_2$.

Fig. 9 shows the FT of k^3-weighted Co K-edge EXAFS oscillations for Co–TiC/SiO$_2$ catalysts. The FT profiles of both Co–TiC/SiO$_2$ showed some similarity to that of Co foil. CF analysis was carried out by using the Co foil as the reference compound; the results are listed in Table 4. The main peak at around 0.2 nm was attributed to Co–Co coordination. CN values (Co–Co) of sc Co–TiC/SiO$_2$ (6.8) and co Co–TiC/SiO$_2$ (6.9) were smaller than that of Co foil (12). It seems that Co on Co–TiC/SiO$_2$ was still dispersed after the high temperature carburization treatment. Taking into account the larger DW
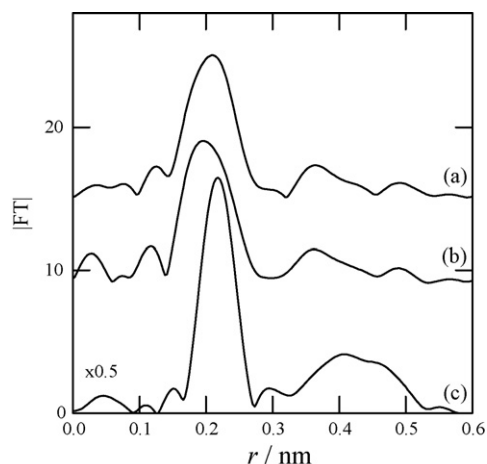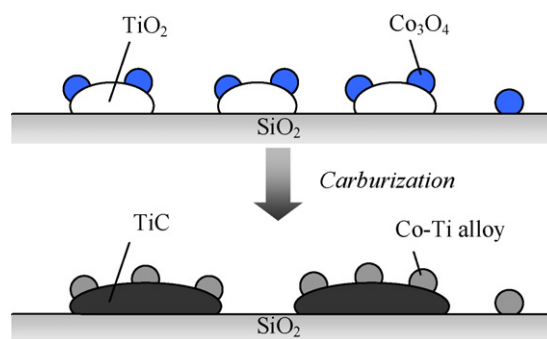
factor for Co–TiC/SiO$_2$ (ca. 0.009 nm), it can be said that the Co lattice of Co–TiC/SiO$_2$ distorted and that the distortion was derived from carbon and Ti dissolved interstitially in the Co lattice. It can be said that TiO$_2$ would be carburized at around the reduced Co site.

From the above results, plausible structures for Co–Ti/SiO$_2$ precursor and Co–TiC/SiO$_2$ catalysts were suggested. Scheme 1 displays the carburization process of sc Co–Ti/SiO$_2$ into sc Co–TiC/SiO$_2$. Scheme 2 displays the carburization process of co Co–Ti/SiO$_2$ into co Co–TiC/SiO$_2$. In the case of sc Co–Ti/SiO$_2$, Co$_3$O$_4$ was formed at the surface of TiO$_2$. During the carburization process, Co oxide was reduced and acted as a carburization center for TiO$_2$ into TiC.

A Co–Ti mixed oxide, such as CoTiO$_3$, was formed at the surface and on the inside of TiO$_2$ on the co Co–Ti/SiO$_2$. Because of the chemical stability of Co–Ti mixed oxide, Co–Ti mixed oxide was hardly reduced during the carburization.

Table 4
Curve-fitting results for Co–Co coordination on Co–TiC/SiO$_2$ catalysts

Sample	Coordination	CN	r (nm)	dE_0 (eV)	DW (nm)
sc Co–TiC/SiO$_2$	Co–Co	6.8	0.251	−16.61	0.0091
co Co–TiC/SiO$_2$	Co–Co	6.9	0.250	−25.46	0.0090
Co foil (model)	Co–Co	12	0.251	0	0.0060
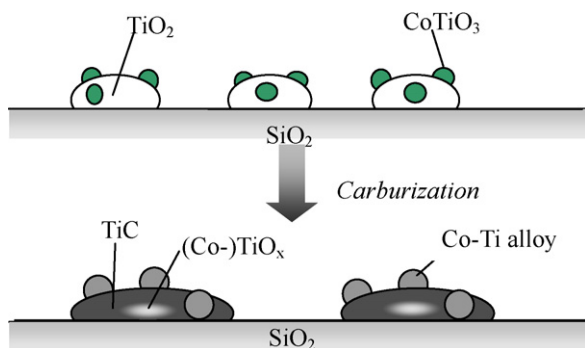
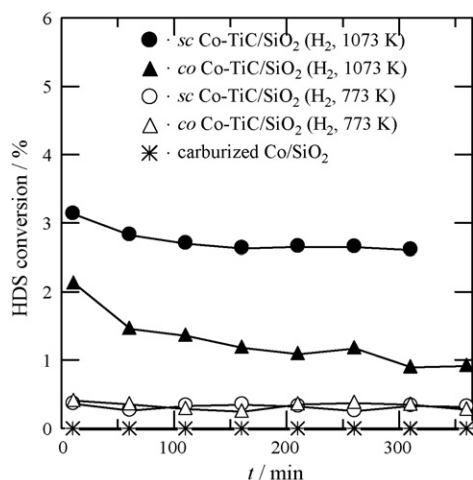Scheme 2. Plausible structure of carburization process from co Co–Ti/SiO₂ into co Co–TiC/SiO₂.

Fig. 10. HDS profiles on Co–TiC/SiO₂ catalysts.

Considering that the carburization of TiO₂ proceeds around reduced Co species, added Co did not effectively work to carburize Ti-oxide on co Co–TiC/SiO₂. So the TiC and Co with a little amount of carbon and Ti dissolved were formed in the lattice and a slight amount of Ti-oxide remained on the co Co–TiC/SiO₂. Since Ti-oxide remained on co Co–TiC/SiO₂, one can conclude that the carburization degree of sc Co–TiC/SiO₂ was better than that of co Co–TiC/SiO₂.

Fig. 10 shows the profile of thiophene HDS conversion on Co–TiC/SiO₂ catalysts. Co–TiC/SiO₂ catalysts were pretreated with H_2 prior to use. Carburized Co/SiO₂ catalyst (without Ti) showed no activity toward thiophene HDS reaction. However, Co–TiC/SiO₂ showed the activity toward thiophene HDS reaction. It was found that reduced Co species show no activity, and that the activity of Co–TiC/SiO₂ depended on TiC.

The activity of Co–TiC/SiO₂ treated with H_2 at 1073 K was greater than that of Co–TiC/SiO₂ treated with H_2 at 773 K. Such results suggested that Ti-oxide and deposited carbon species coated on the surface of TiC were removed by high temperature hydrogen treatment. The activity of sc Co–TiC/SiO₂ was greater than that of co Co–TiC/SiO₂. This trend was similar to the carburization degree of TiC. It was found that the activity toward thiophene HDS reaction was related to the carburization degree of TiC for Co–TiC/SiO₂ catalysts. It was supposed that higher activity could be expected by further increase of the carburization degree.

4. Conclusion

(1) Carburization temperature of Ti-oxide into TiC could be lowered down to 1173 K by addition of Co.
(2) The formation of TiC is affected by carburization temperature rather than by retention time.
(3) Co–Ti/SiO₂ was prepared by use of successive impregnation method (sc) and co-impregnation method (co). Carburization degree of sc Co–TiC/SiO₂ was deeper than that of co Co–TiC/SiO₂.
(4) The activity toward thiophene HDS reaction on sc Co–TiC/SiO₂ was greater than that of co Co–TiC/SiO₂.

References

[1] R. Levy, M. Boudard, Science 181 (1973) 547.
[2] S.T. Oyama, Catal. Today 15 (1992) 179.
[3] C. Loang, W. Ma, Z. Feng, C. Li, Carbon 41 (2003) 1833.
[4] Q. Lu, J. Hu, K. Tang, B. Deng, Y. Qian, G. Zhou, X. Liu, Chem. Phys. Lett. 314 (1999) 37.
[5] S.T. Oyama, J.C. Schlatter, Ind. Eng. Chem. Res. 27 (1988) 1639.
[6] J.G. Chen, Chem. Rev. 96 (1966) 1477.
[7] S.K. Bej, L.T. Thompson, Appl. Catal. A 264 (2004) 141.
[8] A.R.S. Darujati, W.J. Thomson, Appl. Catal. A 296 (2005) 139.
[9] T. Christofoletti, J.M. Assafand, E.M. Assaf, Chem. Eng. J. 106 (2005) 97.
[10] D.C. Lamont, A.J. Gilligan, A.R.S. Darujati, A.S. Chellappa, W.J. Thomson, Appl. Catal. A 255 (2003) 239.
[11] Q. Zhu, B. Zhang, J. Zhao, S. Ji, J. Yang, J. Wang, H. Wang, J. Mol. Catal. A 213 (2004) 199.
[12] K.T. Jung, W.B. Kim, C.H. Rhee, J.S. Lee, Chem. Mater. 16 (2004) 307.
[13] S.K. Bej, C.A. Bennett, L.T. Thomson, Appl. Catal. A 250 (2003) 197.
[14] V.L.S.T. da Silva, M. Schmal, S.T. Oyama, J. Solid State Chem. 123 (1996) 168.
[15] N. Ichikuni, F. Sato, S. Shimazu, T. Uematsu, Top. Catal. 18 (2002) 101.
[16] N. Ichikuni, H. Hachiya, K.K. Bando, S. Shimazu, T. Uematsu, Phys. Scripta T 115 (2005) 807.
[17] G. Jacobs, T.K. Das, P.M. Patterson, J. Li, L. Sanchez, B.H. Davis, Appl. Catal. A 247 (2003) 335.
[18] D. Lützenkirchen-Hecht, M. Wagemaker, P. Keil, A.A. van Well, R. Frahm, Surf. Sci. 538 (2003) 10.
[19] K. Asakura, W.-J. Chun, K. Tohji, Y. Sato, F. Watari, Chem. Lett. 34 (2005) 382.
[20] G.P. Huffman, N. Shah, J. Zhao, F.E. Huggins, T.E. Hoost, S. Halvorsen, J.G. Goodwin Jr., J. Catal. 151 (1995) 17.